

Seismic performance evaluation of staggered wall structures using Fema P695 procedure

Joonho Lee

Graduate student, Department of Architectural Engineering, Sungkyunkwan University, Suwon, Korea

Jinkoo Kim

Professor, Department of Architectural Engineering, Sungkyunkwan University, Suwon, Korea

In this study the seismic performance of six and 12-storey staggered wall structures with a middle corridor is evaluated based on the Fema P695 procedure. The validity of the seismic response factors used for seismic design of the model structures is also evaluated following the procedure. The analysis results of the prototype structures are compared with those of structures with increased coupling beam depth or increased rebar ratio of coupling beams. The adjusted collapse margin ratios of the model structures obtained from incremental dynamic analyses turn out to be larger than the limit states specified in the Fema P695, which implies that the analysis model structures have enough safety margin for collapse against design level earthquakes. It is also concluded that the response modification factor used in the design of the model structures is valid.

Notation

C_0	displacement coefficient of equivalent SDOF system	$TH_{1,i}$	record i of horizontal component 1
\hat{C}	median structural capacity, associated with the limit state	$TH_{2,i}$	record i of horizontal component 2
\hat{D}	median structural demand	V_{max}	maximum base shear
EI	bending rigidity	W	building weight
g	gravitational constant	β_{DR}	design requirements related uncertainty
K_0	initial stiffness of concrete	β_{MDL}	modeling uncertainty
K_h	post-yield stiffness of concrete	β_{RTR}	record-to-record uncertainty
L	beam length	β_{TD}	test data related uncertainty
M_{pr}	probable flexural strength	β_{TOT}	total system collapse uncertainty
M_u	ultimate bending moment	δ_u	ultimate roof drift displacement
M_y	yield bending moment	$\delta_{y,eff}$	effective yield roof drift displacement
Median($PGV_{PEER,i}$)	median of $PGV_{PEER,i}$	θ_R	rotation angle right before strength drop
NM_i	normalisation factor of i th record	θ_L	rotation angle right after strength drop
$NTM_{1,i}$	normalised i th record of horizontal component 1	μ_T	period-based ductility factor for a given structure
$NTM_{2,i}$	normalised i th record of horizontal component 2	$\Phi[\cdot]$	standard normal probability integral
$PGV_{PEER,i}$	peak ground velocity of the i th record		
S_{cr}	spectral acceleration		
S_{MT}	maximum considered earthquake intensity		
\hat{S}_{CT}	median collapse intensity		
SD_{CT}	median spectral displacement of collapse-level earthquake		
SD_{MT}	median spectral displacement of MCE-level earthquake		
T	fundamental period defined by equation 5-5 of Fema P695 and		
T_1	fundamental period of the model computed using eigenvalue analysis		

Introduction

Staggered wall structures are structural systems for reinforced concrete (RC) residential buildings in which storey-high walls extend across the entire width of the buildings. By staggering the locations of the walls on alternate floors, large clear areas are created on each floor. Floor slabs span only half the wall spacing. The staggered walls can be pierced for openings or corridors. A similar system, the staggered truss system, has been applied in steel structures. The system is best suited for rectangular plan buildings with permanent interior partitions, but can easily be adapted to other plan shapes. By extending the walls beyond the column lines, a variety of balcony arrangements can be achieved. The system was first proposed by Fintel (1968), who conducted experiments on a half-scale staggered wall structure subjected to gravity load. He also carried out a comparative study of three different structure

systems for residential buildings to investigate the cost effectiveness of staggered wall systems. It was observed that, compared with shear wall structures and flat plate structures with the same configuration, the staggered wall systems can be designed with the smallest amount of concrete for the same design load and therefore this system results in the lightest structure. It was concluded that staggered wall systems are very competitive with the conventional form of construction and in many cases will be more economical. Mee *et al.* (1975) carried out shaking table tests of 1/15 scaled models for the staggered wall systems. It was found that the consistent mass analysis gave a reasonable estimation of the dynamic behaviour of the system. Kim and Jun (2011) evaluated the seismic performance of partially staggered wall apartment buildings using non-linear static and dynamic analysis, and compared the results with those of conventional shear wall system apartment buildings. They found that the structure with a partially staggered wall system satisfied the collapse prevention performance objective required by Fema 356 (Fema, 2000) and thus was considered to have enough capacity for design level seismic load.

Fema P695 (Fema, 2009) recommends a methodology for quantifying building system performance and response parameters for use in seismic design. The methodology achieves the primary life safety performance objective by requiring an acceptably low probability of collapse of the seismic-force-resisting system when subjected to maximum considered earthquake (MCE) ground motions. The methodology consists of a framework for establishing seismic performance factors that involves development of detailed system design information and probabilistic assessment of collapse risk. It utilises non-linear analysis techniques, and explicitly considers uncertainties in ground motion, modelling, design and test data. The technical approach is a combination of incremental non-linear dynamic analyses and fragility analyses. In the present study, the seismic performances of six and 12-storey staggered wall structures were evaluated based on the Fema P695 procedure. Non-linear static analyses were performed to obtain the ductility capacity and the spectral shape factor (SSF) of model structures. Incremental dynamic analyses of the model structures were carried out using the 22 pairs of scaled records to compute the collapse margin ratios of the model structures from the median collapse intensity and the MCE intensity. The validity of the seismic performance factor used for seismic design was also evaluated following the Fema P695 procedure. The analysis results of the prototype structures designed per current design code were compared with those of the structures with increased coupling beam depth or increased coupling beam rebar ratio to investigate the effect of the retrofit. Seismic fragility analyses were carried out to compare the probability of failure for a given earthquake intensity.

Design of analysis model structures

Configuration of the analysis model structures

In the staggered wall systems the storey-high RC walls that span the width of the building are located along the short direction in a staggered pattern. The floor system spans from the top of one

staggered wall to the bottom of the adjacent wall, serving as a diaphragm, and the staggered walls with attached slabs resist gravity as well as lateral loads as H-shaped storey-high deep beams (Fintel, 1968). The horizontal load is transferred to the staggered walls through diaphragm action of floor slabs, as shown in Figure 1. The figure shows the flow of horizontal shear force from the staggered walls above to the columns and staggered walls below through the floor diaphragm. With RC walls located at alternate floors, flexibility in spatial planning can be achieved compared with conventional structures with vertically continuous shear walls. Figure 2 shows the deformation of the staggered wall systems with middle corridors subjected to lateral load. As the exterior columns and the link beams above the openings along the corridors are weaker and more flexible than the storey-high walls, large deformation is concentrated in the beams and columns. This leads to shear mode behaviour when the system is subjected to lateral load. Figure 3 shows the structural configuration of the model structures. Columns and beams are located along the longitudinal perimeter of the structures, providing a full width of column-free area within the structure. Along the longitudinal direction, the column-beam combination resists lateral load as a moment-resisting frame.

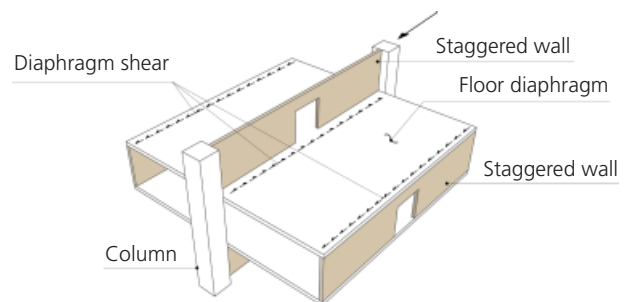


Figure 1. Lateral load path of a staggered wall structure

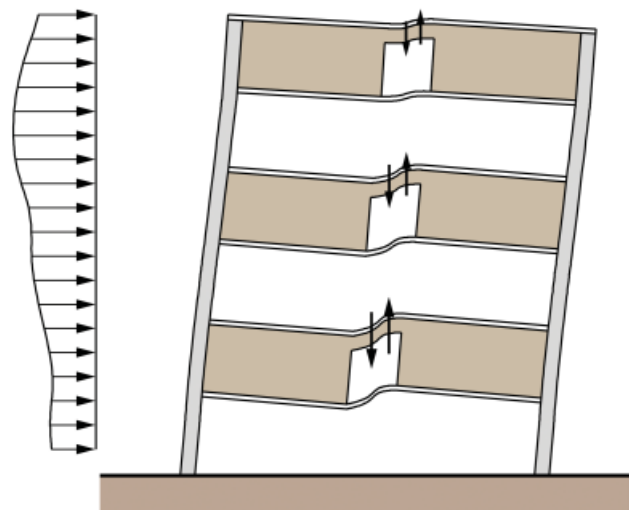


Figure 2. Lateral deformation of staggered wall structures with middle corridors

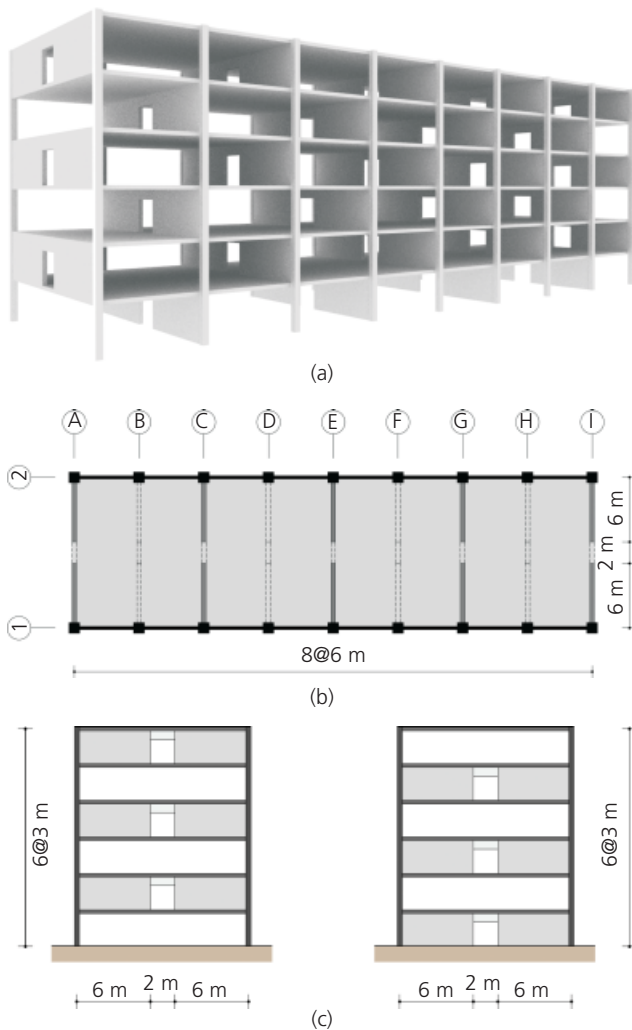


Figure 3. Configuration of the six-storey staggered wall structure used in the analysis: (a) three-dimensional view; (b) plan view; (c) side view

Structural design of analysis model structures

The staggered truss or staggered wall systems have not been considered as one of the basic seismic-force-resisting systems in most design codes. Fema 450 (Fema, 2003) requires that lateral systems that are not listed as the basic seismic-force-resisting systems shall be permitted if analytical and test data are submitted to demonstrate the lateral force resistance and energy dissipation capacity. The American Institute of Steel Construction *Steel Design Guide 14* (AISC, 2002) recommends the response modification factor of 3.0 for seismic design of staggered truss system buildings; however, the other seismic behaviour factors, such as overstrength and ductility factors, to define inelastic behaviour of the structure, are not specified.

To evaluate the seismic performance of staggered wall system structures, six and 12-storey structural models were designed and were named as SWC06 and SWC12, respectively. The model

structures were designed as per the ACI 318-05 (ACI, 2005) using the seismic loads specified in the IBC 2009 (ICC, 2009). The dead load was estimated to be 7 kN/m^2 including the weight of 210 mm thick concrete slab and the floor panel heating system, and the live load of 2 kN/m^2 was used for structural design. The design seismic load was computed based on the design spectral response acceleration parameters $S_{DS} = 0.31 g$ and $S_{D1} = 0.13 g$. This corresponds to the design seismic load in the Los Angeles area with site class B, which is a rock site. As the response modification factor for a staggered wall system is not specified in the current design codes, the response modification factor of 3.0 was used in the structural design of the staggered wall systems, which is generally used for structures to be designed without consideration of seismic detailing. Along the longitudinal direction the structures were designed as ordinary moment-resisting frames with R -factor of 3.0. The ultimate strength of concrete is 27 MPa and the tensile strength of rebars is 400 MPa. The thickness of the staggered walls is 20 cm throughout the storeys, and the connecting beams have dimensions of $600 \times 200 \text{ mm}$. D13 rebars are placed in the walls at an interval of 200 mm in both horizontal and vertical directions. The thickness of the floor slabs is 210 mm, which is the minimum thickness required for wall-type apartment buildings in Korea to prevent transmission of excessive noise and vibration through the floors. The sizes of columns vary from $600 \times 600 \text{ mm}$ to $520 \times 520 \text{ mm}$ along the height in the six-storey structure, and from 760×760 to 540×540 in the 12-storey structure. As the coupling beams located between two wall panels are considered to be the weakest links when subjected to lateral loads, two more models were prepared with the coupling beams strengthened. To observe the effect of strengthening coupling beams on the overall seismic performance of the staggered wall structures, the depth of the coupling beams of the prototype structures was increased to 75 cm (SWC06_A and SWC12_A). Also prepared are the structures with their rebar ratios of coupling beams arbitrarily increased by 50% (SWC06_B and SWC12_B).

Modelling for analysis

Non-linear analyses of the model structures were carried out using the program code Perform 3D (2006). The force–displacement relationship of the columns was modelled using the ‘Fema column, concrete type’ elements provided in Perform 3D, which is illustrated in Figure 4(a). The interaction of bending moment and axial force was considered by the P-M-M yield surface presented in Figure 4(b). The staggered walls were modelled by the ‘shear wall’ fibre elements. The stress–strain relationship of concrete fibre elements was defined as trilinear lines, as shown in Figure 5(a) based on the material model of Paulay and Priestley (1992) without confinement effect. In the model the ultimate strength and yield strength of concrete are 27 MPa and 18 MPa, respectively, and the residual strength is defined as 20% of the ultimate strength. The strain at the ultimate strength is 0.002, and the ultimate strain is defined as 0.004. The tensile strength of concrete is neglected. In Figure 5(a), the initial stiffness of concrete K_0 is 2778.2 kN/m^2 , and the post-yield stiffness K_h is determined as

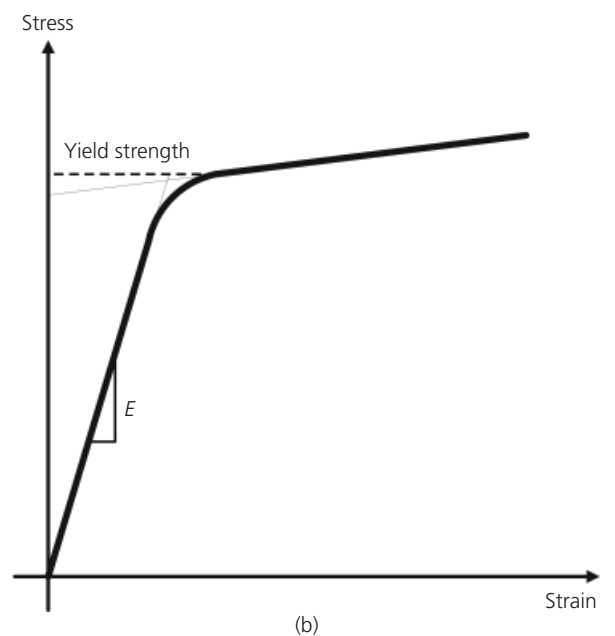
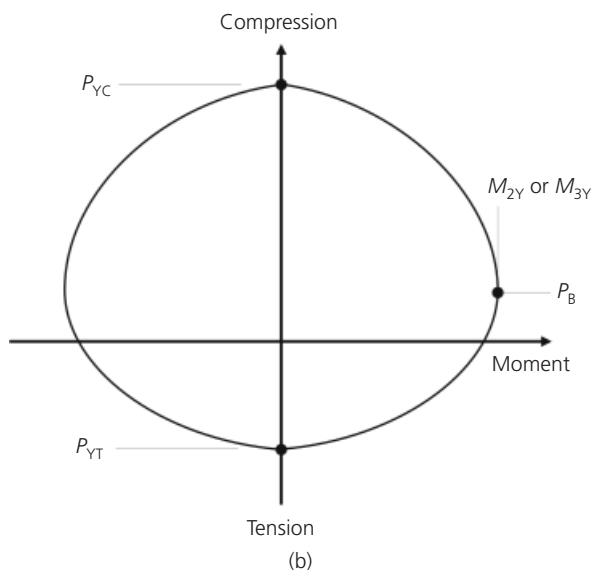
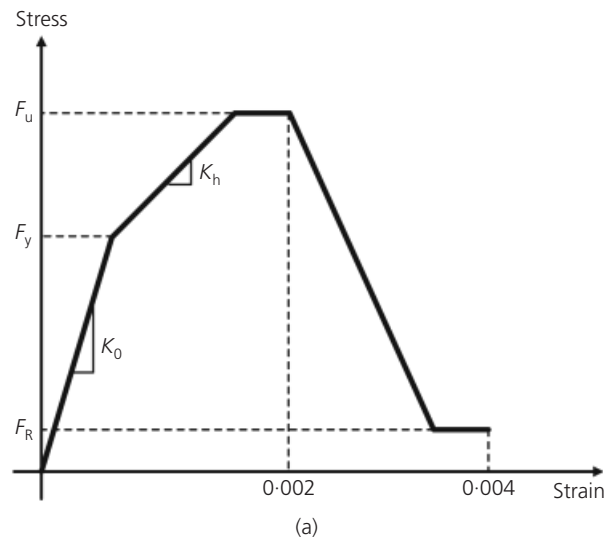
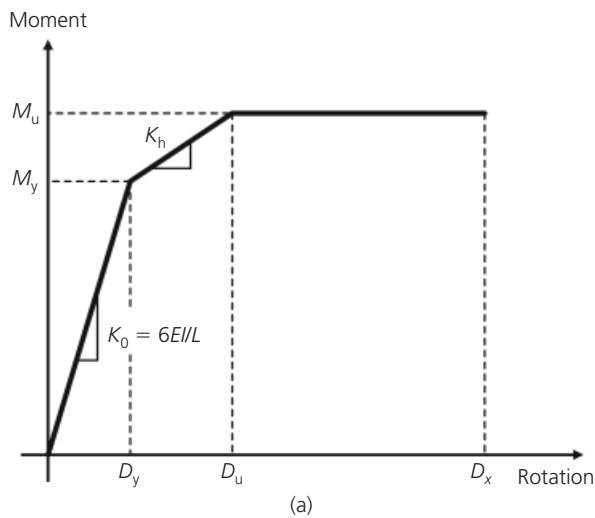


Figure 4. Force–deformation relationship of columns: (a) moment–rotation relationship; (b) triaxial P-M-M yield surface

Figure 5. Stress–strain relationship of shear wall fibre elements: (a) concrete; (b) reinforcing steel

30% of K_0 , which is 833.5 kN/m^2 . The descent stiffness of the post-failure line is 1200 kN/cm^2 . The reinforcing steel fibre elements were modelled with bilinear lines, as depicted in Figure 5(b). Overstrength factors of 1.5 and 1.25 were used for the modelling of concrete and reinforcing steel, respectively.

The analysis model for connecting beams located between the two staggered walls is composed of two end-rotation-type moment hinges and a middle shear hinge, as shown in Figure 6(a). The moment hinge was defined based on ASCE/SEI 41-06 (ASCE, 2005) (Figure 6(b)), and the shear hinge was defined based on Englekirk (2003). In Figure 6(b) the initial stiffness K_0 of the columns and the coupling beams was determined from $6EI/L$ of the members, and the post-yield stiffness K_h was determined from the difference between M_y and M_u divided by 70% of the inelastic deformation capacity defined in ASCE/SEI

41-06. The descent stiffness of the post-failure line was determined in such a way that θ_R is 1.05 times θ_L . Figure 6(b) was modified as follows to illustrate the descent stiffness of the post-failure line more realistically. The probable flexural strength, M_{pr} , is obtained from the nominal moment strength multiplied by the overstrength factor, and the shear strength is computed as follows

$$1. \quad V_u = \frac{2M_{pr}}{L}$$

As the shear wall element has no in-plane rotational stiffness at its nodes, a beam element was embedded in the wall as shown in

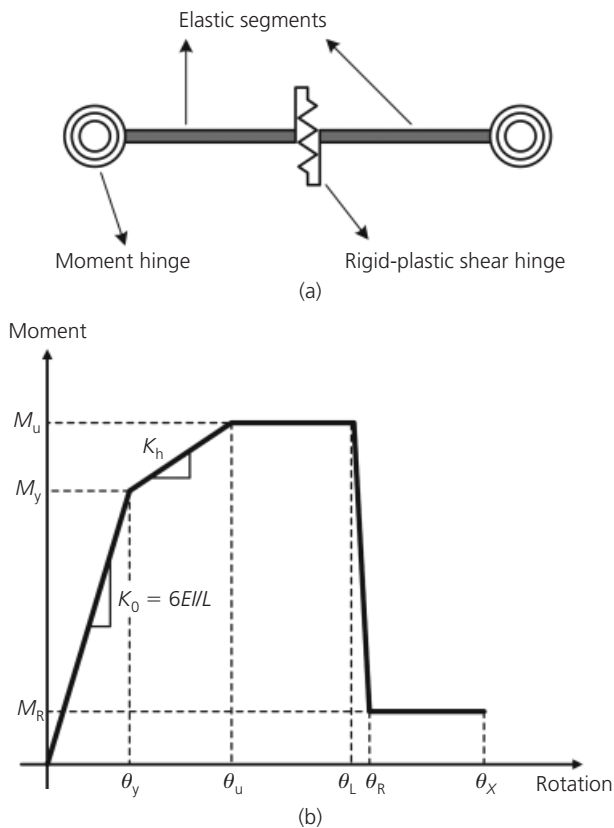


Figure 6. Analysis modelling of coupling beams: (a) three-hinge model composed of two end moment hinges and a centre shear hinge; (b) moment–rotation relationship

Figure 7 to specify a moment-resisting connection between a beam and a wall.

Fema P695 procedure for seismic performance evaluation

Scaling of ground motion record sets

Fema P695 provides 22 pairs of earthquake records through the PEER-NGA (2013) database for non-linear analysis of structures. Ground motions are scaled to represent a range of earthquake intensities up to collapse level ground motions. The individual records in each set are normalised by their respective peak ground velocities first. This step is intended to remove unwarranted

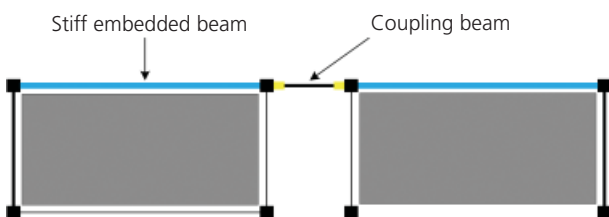


Figure 7. Installation of embedded beams at the top of staggered walls

variability between records due to inherent differences in event magnitude, distance to source, source type and site conditions, without eliminating record-to-record variability. The following formulae presented in the Fema P695 Appendix A.8 define the normalisation factor of the i th record, NM_i , and calculation of normalised horizontal components of the i th record, respectively

$$2a. \quad NM_i = \frac{\text{Median}(PGV_{PEER,i})}{PGV_{PEER,i}}$$

$$2b. \quad NTH_{1,i} = NM_i \times TH_{1,i}, \quad NTH_{2,i} = NM_i \times TH_{2,i}$$

where $PGV_{PEER,i}$ is the peak ground velocity of the i th record, $\text{Median}(PGV_{PEER,i})$ is the median of $PGV_{PEER,i}$, $NM_{1,i}$ is the normalised i th record of horizontal component 1, $NM_{2,i}$ is the normalised i th record of horizontal component 2, $TH_{1,i}$ is the record i of the horizontal component 1, and $TH_{2,i}$ is the record i of the horizontal component 2. Next normalised ground motions are collectively scaled (or anchored) to a specific ground motion intensity such that the median spectral acceleration of the record set matches spectral acceleration at the fundamental period of the structure being analysed.

Spectral shape factors

Baker and Cornell (2006) showed that rare ground motions have a distinctive spectral shape that differs from the shape of the design spectrum used for structural design. As selecting a unique set of ground motions that have the appropriate shape for each site, hazard level and structural period of interest is not feasible in practice, Fema P695 recommends using the SSFs, which depend on fundamental period and period-based ductility to adjust collapse margin ratios. Using the two factors, the SSF of a structure can be found in Table 7-1 of Fema P695.

A non-linear static (pushover) analysis is performed to check non-linear behaviour of the model to verify that all elements have not yielded at the point that a collapse mechanism develops in the structure. The ductility capacity is determined from pushover analysis results, and the SSF, is determined based on the ductility capacity and the fundamental period. Figure 8 illustrates the spectral acceleration plotted against spectral displacement relationship of a structure showing the seismic performance factors as defined by Fema P695. Instead of the conventional ductility factor, the period-based ductility is recommended to consider the effect of elongation of natural period prior to collapse. The period-based ductility factor for a given structure, μ_T , is defined as the ratio of ultimate roof drift displacement, δ_u , to the effective yield roof drift displacement $\delta_{y,eff}$

$$3. \quad \mu_T = \frac{\delta_u}{\delta_{y,eff}}$$

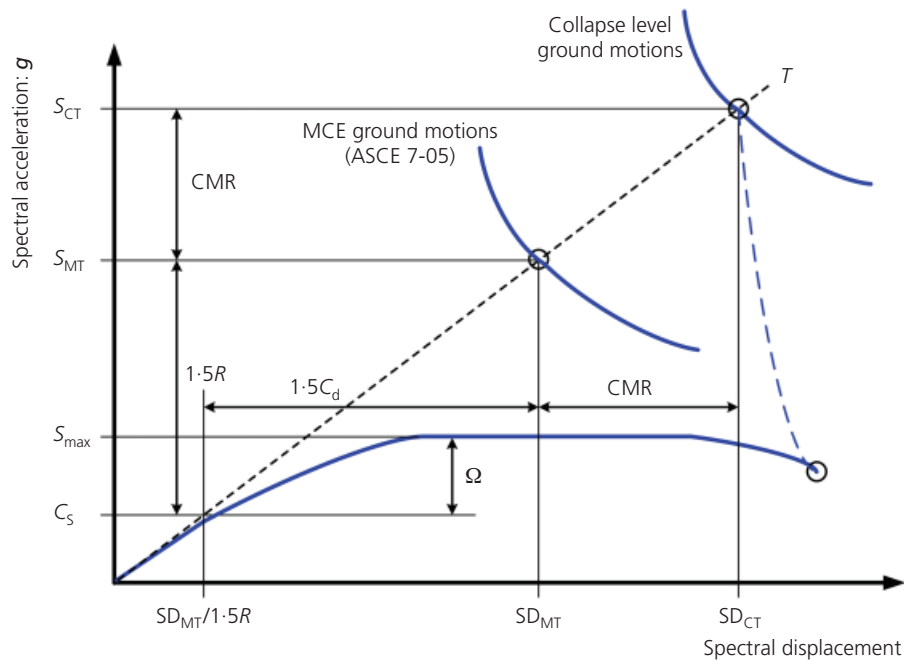


Figure 8. Illustration of seismic performance factors

The effective yield roof drift displacement is given by the following formula in Fema P695

$$4. \quad \delta_{y, \text{eff}} = C_0 \frac{V_{\text{max}}}{W} \left[\frac{g}{4\pi^2} \right] [\max(T, T_1)]^2$$

where C_0 relates fundamental-mode (single degree of freedom) displacement to roof displacement, V_{max}/W is the maximum base shear normalized by building weight, g is the gravity constant, T is the fundamental period defined by Equation 5-5 of Fema P695, and T_1 is the fundamental period of the model computed using eigenvalue analysis. The period-based ductility coefficient is used to determine the SSF. The SSF obtained in this way is multiplied by the collapse margin ratio (CMR) to compute the adjusted collapse margin ratio (ACMR).

Collapse margin ratio

A non-linear incremental dynamic analysis of the model structure is performed separately for each scaled record of the record set. If less than one half of the records cause collapse, then the trial design meets the collapse performance objective, and the building has an acceptably low probability of collapse for MCE ground motions. Non-linear dynamic analyses are generally required to establish the median collapse capacity and CMR for each of the analysis models. The ratio between the median collapse intensity, \hat{S}_{CT} , and the MCE intensity, S_{MT} , is defined as the CMR, which is the primary parameter used to characterise the collapse safety of the structure

$$5. \quad \text{CMR} = \frac{\hat{S}_{CT}}{S_{MT}} = \frac{SD_{CT}}{SD_{MT}}$$

The median collapse spectral intensity, \hat{S}_{CT} , was taken as the median spectral acceleration at the code-based structural period, T , and the analyses were discontinued as soon as half of the records were observed to result in collapse.

Determination of the collapse margin ratio for each model is expected to require approximately five analyses of varying intensity for each component of the 22 pairs of earthquake ground motion records. Ground motion intensity is defined based on the median spectral intensity of the far-field record set, measured at the fundamental period of the structure. The procedure for conducting non-linear response history analyses is based on the concept of incremental dynamic analysis (IDA) (Vamvatsikos and Cornell, 2002), in which each ground motion is scaled to increasing intensities until the structure reaches a collapse point.

Total system collapse uncertainty

Acceptable values of adjusted collapse margin ratio are based on the total system collapse uncertainty, β_{TOT} , and established values of acceptable probabilities of collapse. They are based on the assumption that the distribution of collapse level spectral intensities is lognormal, with a median value, \hat{S}_{CT} , and a lognormal standard deviation equal to the total system collapse uncertainty, β_{TOT} , which is computed as follows

$$6. \quad \beta_{TOT} = \sqrt{\beta_{RTR}^2 + \beta_{DR}^2 + \beta_{TD}^2 + \beta_{MDL}^2}$$

The total system collapse uncertainty, β_{TOT} , is a function of record-to-record uncertainty (β_{RTR}), design requirements related uncertainty (β_{DR}), test data related uncertainty (β_{TD}) and modelling uncertainty (β_{MDL}). Quality ratings for design requirements, test data and non-linear modelling are translated into quantitative values of uncertainty based on the following scale: (A) superior, $\beta = 0.20$; (B) good, $\beta = 0.30$; (C) fair, $\beta = 0.45$; and (D) poor, $\beta = 0.65$. Values of total system collapse uncertainty, β_{TOT} , are provided in Table 7-2 of the Fema P695. Table 7-3 of the Fema P695 provides acceptable values of adjusted collapse margin ratio, $ACMR_{10\%}$ and $ACMR_{20\%}$, based on total system collapse uncertainty and values of acceptable collapse probability, taken as 10% and 20%, respectively. Lower values of acceptable collapse probability and higher levels of collapse uncertainty result in higher required values of adjusted collapse margin ratio.

Median collapse intensity and collapse fragility

Collapse is judged to occur either directly from dynamic analysis results (dynamic instability or excessive lateral displacements) or indirectly through component limit state criteria. Using collapse data obtained from non-linear dynamic analyses, a collapse fragility can be defined through a cumulative distribution function, which relates the ground motion intensity to the probability of collapse (Ibarra *et al.*, 2002). The lognormal distribution is defined by two parameters, which are the median collapse intensity, \hat{S}_{CT} , and the standard deviation of the natural logarithm, β . The median collapse capacity corresponds to a 50% probability of collapse. The slope of the lognormal distribution is measured by β , and reflects the variability or uncertainty in results. \hat{S}_{CT} can be obtained by scaling all the records in the far-field record set to the MCE intensity, S_{MT} , and then by increasing intensity until one half of the scaled ground motion records cause collapse. The lowest intensity at which one half of the records cause collapse is the median collapse intensity, \hat{S}_{CT} .

Fragility curves show the probability of a system reaching a limit state as a function of some measure of seismic intensity. In this study pseudo spectral acceleration was used as the seismic intensity measure. The state of dynamic instability was considered as the limit state for failure. The seismic fragility is described by the conditional probability that the structural capacity, C , fails to resist the structural demand, D , given the seismic intensity hazard, SI , and is modelled by a lognormal cumulative distribution function as follows (Ellingwood *et al.*, 2007)

$$7. \quad P[C < D | SI = x] = 1 - \Phi \left[\frac{\ln(\hat{C}/\hat{D})}{\beta_{TOT}} \right]$$

where $\Phi[\cdot]$ is the standard normal probability integral, \hat{C} is the

median structural capacity, associated with the limit state, \hat{D} is the median structural demand, and β_{TOT} is the total system collapse uncertainty. The lognormal collapse fragility is defined by the median collapse intensity, \hat{S}_{CT} , and the standard deviation of the natural logarithm. The median collapse capacity corresponds to a 50% probability of collapse.

Seismic performance evaluation of model structures

Figure 9 shows the pushover curves of the six and 12-storey model structures. In addition to the prototype structures (SWC06 and SWC12), the structures with increased coupling beam depth

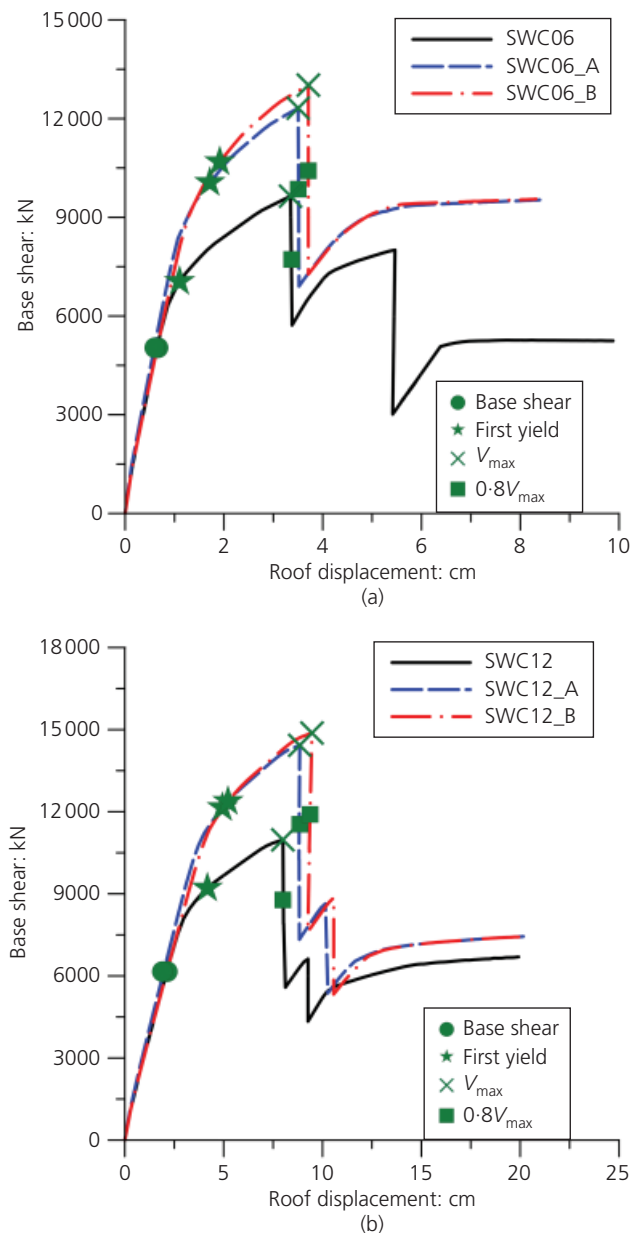


Figure 9. Pushover curves of staggered wall analysis model structures: (a) six storey; (b) 12 storey

(SWC06_A and SWC12_A) and the structures with increased coupling beam rebar ratio (SWC06_B and SWC12_B) were analysed. It can be observed that the retrofitted structures show significantly higher strength than those of the prototype structures. The strengths of the structures retrofitted in two different ways are similar to each other. Important points such as the design base shear, first yield, maximum strength and the strength corresponding to 80% of the maximum strength are marked on the pushover curves. Table 1 shows the overstrength factors and the period-based ductility factors obtained by using Equations 3 and 4, respectively.

Incremental dynamic analyses of the model structures were carried out using the 22 pairs of scaled records to compute the CMRs of the model structures. Damping ratios of 5% were used for all vibration modes and the pinching effect was not considered in the dynamic analysis. The spectral acceleration plotted against maximum inter-storey drift ratio obtained from incremental dynamic analyses of the six model structures using the 44 earthquake records are presented in Figure 10(a)–10(f). In the figures the 22 IDA curves that showed dynamic instability of the model structures are presented in black. The grey curves represent the IDA curves that did not reach the state of dynamic instability. The median collapse intensity or the spectral acceleration (\hat{S}_{CT}) at which the 22nd dynamic instability of each model structure was initiated was determined from the IDA curves and is presented in Table 2. The state of dynamic instability was defined as the point at which the stiffness of the structure decreased to 20% of the initial stiffness (Vamvatsikos and Cornell, 2002). It can be observed that the median collapse intensity, \hat{S}_{CT} , increased by 6% and 8%, respectively, in the six and 12-storey structures when the depth of the coupling beams was increased from 600 mm to 750 mm. In the structures retrofitted by increasing the rebar ratio of the coupling beams, the collapse intensity increased by 11% and 16% in the six and 12-storey structures, respectively. The collapse margin ratio, which is the primary parameter used to characterise the collapse safety of the structure, was obtained from the ratio between the median collapse intensity, \hat{S}_{CT} , and the MCE intensity, S_{MT} , as defined in Equation 5.

The SSFs of the model structures were obtained in the Table 7-1

Analysis model	Overstrength factor: Ω	Period-based ductility: μ_T
SWC06	1.915	4.445
SWC06_A	2.446	4.279
SWC06_B	2.585	3.649
SWC12	1.782	3.305
SWC12_A	2.343	3.201
SWC12_B	2.417	3.005

Table 1. Overstrength factor and period-based ductility of model structures

of Fema P695 using the natural periods and period-based ductility coefficients presented in Table 1. The SSF obtained in this way was multiplied to the CMR to compute the ACMR; these values are shown in Table 2. ACMR increased by the same proportion as the increase of CMR. Among the model structures the collapse margin was larger in the 12-storey structures and in the structures with their coupling beams strengthened.

The total system collapse uncertainty, β_{TOT} , of the model structures was determined based on the assumption that the qualities of design requirements and model quality were ‘good’. Considering the fact that sufficient test data have not yet been provided regarding the seismic capacity of staggered wall structures, the quality of test data was considered to be ‘poor’. Using Table 7-2b of Fema P695, which is shown in Table 3 of the present paper, the total system collapse uncertainty, β_{TOT} , was obtained as 0.7. From Table 7-3 of Fema P695, part of which is shown in Table 4 of the current paper, the acceptable value of the adjusted collapse margin ratio corresponding to the collapse probability of 20% ($ACMR_{20\%}$) was found to be 1.8 for the total system collapse uncertainty of 0.7. It can be observed in Table 2 that the computed ACMRs for all model structures range from 3.5 to 4.7, so are greater than the acceptable value of 1.8. This implies that the analysis model structures have a higher margin for collapse than required by Fema P695 and that the response modification factor used in the seismic design of the model structures is acceptable.

Figure 11 depicts the fragility curves of the model structures obtained using the median collapse intensity, \hat{S}_{CT} , and the total system collapse uncertainty, β_{TOT} , computed from the incremental dynamic analysis results of the 22 pairs of ground motions. The spectral acceleration corresponding to the MCE ground motion and the spectral acceleration corresponding to the 50% probability of collapse, were also indicated on the figures. It can be observed that the probability of collapse at MCE level earthquake is less than 10% and the margin for collapse is significantly larger than the acceptable values of adjusted collapse margin ratio, which is 1.8. In the staggered wall structures retrofitted by increasing the depth of the coupling beams, the spectral accelerations corresponding to the collapse probability of 0.5 slightly increased. This implies that the margins for collapse against MCE level earthquakes increased due to the results of retrofit.

Conclusions

In this study the seismic performance of six and 12-storey staggered wall structures was evaluated based on the Fema P695 procedure. Non-linear static (pushover) analyses were performed to obtain the ductility capacity and the SSF of model structures. Incremental dynamic analyses of the model structures were carried out using the 22 pairs of scaled records to compute the collapse margin ratios of the model structures from the ratio between the median collapse intensity, \hat{S}_{CT} , and the MCE intensity, S_{MT} . The analysis results of the prototype structures

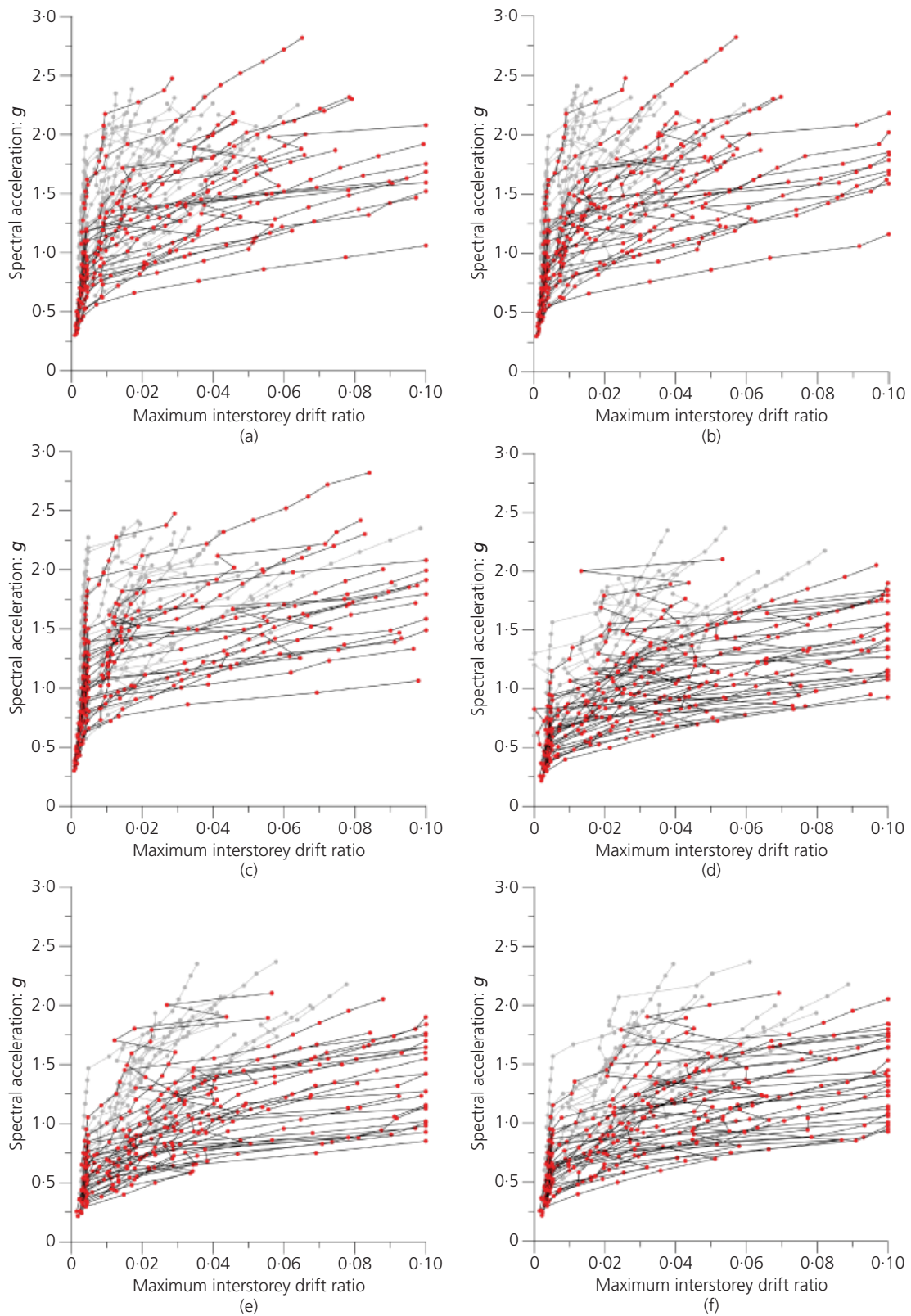


Figure 10. IDA results of analysis model structures: (a) SWC06; (b) SWC06_A; (c) SWC06_B; (d) SWC12; (e) SWC12_A; (f) SWC12_B

Analysis model	\hat{S}_{CT}	CMR	SSF	ACMR
SWC06	1.809	3.289	1.094	3.598
SWC06_A	1.909	3.471	1.093	3.794
SWC06_B	2.009	3.653	1.093	3.993
SWC12	1.229	3.687	1.096	4.041
SWC12_A	1.329	3.987	1.094	4.362
SWC12_B	1.429	4.287	1.090	4.673

Table 2. Adjusted collapse margin ratio (ACMR) of model structures

Quality of test data	Quality of design requirements			
	A, superior	B, good	C, fair	D, poor
A, superior	0.475	0.500	0.575	0.675
B, good	0.500	0.525	0.600	0.700
C, fair	0.575	0.600	0.675	0.750
D, poor	0.675	0.700	0.750	0.825

Table 3. Total system collapse uncertainty (β_{TOT}) for model quality B, good and period-based ductility $\mu_T \geq 3$

Total system collapse uncertainty	Collapse probability				
	5%	10% (ACMR _{10%})	15%	20% (ACMR _{20%})	25%
∴	∴	∴	∴	∴	∴
0.650	2.91	2.30	1.96	1.73	1.55
0.675	3.04	2.38	2.01	1.76	1.58
0.700	3.16	2.45	2.07	1.80	1.60
0.725	3.30	2.53	2.12	1.84	1.63
0.750	3.43	2.61	2.18	1.88	1.66
∴	∴	∴	∴	∴	∴

Table 4. Acceptable values of adjusted collapse margin ratio

designed as per current design code were compared with those of the structures with increased coupling beam depth or increased coupling beam rebar ratio to investigate the effect of the retrofit.

It was observed in the pushover analysis results that the retrofitted structures retained significantly higher strength than those of the prototype structures. The incremental dynamic analysis results showed that the adjusted collapse margin ratios of the model structures were significantly larger than the limit states specified in the Fema P695. Among the model structures the collapse margin was larger in the 12-storey structures and in the structures

with their coupling beams strengthened. Based on the analysis results it was concluded that the staggered wall analysis model structures have enough safety against design level earthquakes, and that the seismic response factors used for design of model structures are valid.

Acknowledgement

This work (no. 2011-0015734) was supported by the mid-career researcher program through a National Research Foundation grant funded by the Korea Ministry of Education, Science and Technology.

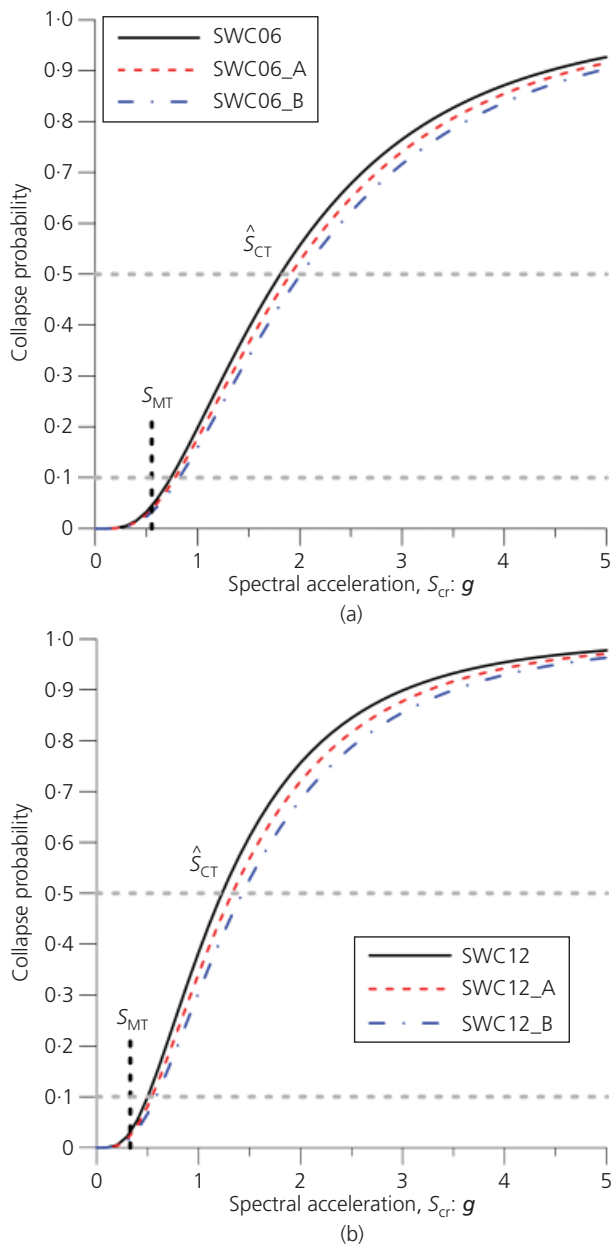


Figure 11. Fragility curves of model structures: (a) SWC06; (b) SWC12

REFERENCES

ACI (American Concrete Institute) (2005) ACI 318-05: Building code requirements for structural concrete. American Concrete Institute, Farmington Hills, MI, USA.

AISC (American Institute of Steel Construction) (2002) *Steel Design Guide 14: Staggered Truss Framing System*. American Institute of Steel Construction, Chicago, USA.

ASCE (2005) ASCE/SEI 7-05: Minimum design loads for buildings and other structures. American Society of Civil Engineers, Reston, VA, USA.

Baker JW and Cornell CA (2006) Spectral shape, epsilon and

record selection. *Earthquake Engineering and Structural Dynamics* **34**(10): 1193–1217.

Ellingwood BR, Celik OC and Kinali K (2007) Fragility assessment of building structural systems in Mid-America. *Earthquake Engineering and Structural Dynamics* **36**(13): 1935–1952.

Englekirk R (2003) *Seismic Design of Reinforced and Precast Concrete Buildings*. Wiley, Hoboken, NJ, USA.

Fema (Federal Emergency Management Agency) (2000) Fema 356: Prestandard and commentary for the seismic rehabilitation of buildings. Federal Emergency Management Agency, Washington, DC, USA.

Fema (2003) Fema 450: *NEHRP Recommended Provisions for Seismic Regulations for New Buildings and Other Structures*. Federal Emergency Management Agency, Washington, DC, USA.

Fema (2009) Fema P695: *Quantification of Building Seismic Performance Factors*. Federal Emergency Management Agency, Washington, DC, USA.

Fintel M (1968) Staggered transverse wall beams for multistory concrete buildings. *ACI Journal* **65**(5): 366–378.

Ibarra L, Medina R and Krawinkler H (2002) Collapse assessment of deteriorating SDOF systems. *Proceedings of the 12th European Conference on Earthquake Engineering, London*. Elsevier, Amsterdam, the Netherlands, paper no. 665.

ICC (International Code Council) (2009) IBC 2009: International building code. International Code Council, Falls Church, VA, USA.

Kim J and Jun Y (2011) Seismic performance evaluation of partially staggered wall apartment buildings. *Magazine of Concrete Research* **63**(1): 1–13.

Mee AL, Jordaan IJ and Ward MA (1975) Dynamic response of a staggered wall-beam structure. *Earthquake Engineering and Structural Dynamics* **3**(4): 353–364.

Paulay T and Priestley MJN (1992) *Seismic Design of Reinforced Concrete and Masonry Building*. Wiley, Hoboken, NJ, USA.

PEER-NGA (2013) PEER-NGA database. Pacific Earthquake Engineering Research Center, University of California, Berkeley, CA, USA.

Perform 3D (2006) *Nonlinear Analysis and Performance Assessment for 3D Structures – User Guide*. Computers and Structures, Berkeley, CA, USA.

Vamvatsikos D and Cornell CA (2002) Incremental dynamic analysis. *Earthquake Engineering and Structural Dynamics* **31**(3): 491–514.

WHAT DO YOU THINK?

To discuss this paper, please submit up to 500 words to the editor at www.editorialmanager.com/macr by 1 March 2014. Your contribution will be forwarded to the author(s) for a reply and, if considered appropriate by the editorial panel, will be published as a discussion in a future issue of the journal.